

Origins of switching field distributions in perpendicular magnetic nanodot arrays

Justin M. Shaw,^{a)} William H. Rippard, and Stephen E. Russek
National Institute of Standards and Technology, Boulder, Colorado 80305

Timothy Reith and Charles M. Falco
College of Optical Sciences, University of Arizona, Tucson, Arizona 85721

(Received 16 November 2006; accepted 17 November 2006; published online 19 January 2007)

We studied the reversal properties of perpendicularly magnetized Co/Pd nanodots from 100 to 50 nm in diameter fabricated using electron beam lithography. Polycrystalline Co/Pd multilayers show considerable differences in the switching field distribution (SFD) depending on the seed layer used. With a Ta seed layer, we reduced the SFD to approximately 5% of the average switching field. To rule out effects of grain boundaries, we also fabricated nanodot arrays from epitaxial Co/Pd superlattices. Although significant improvement in SFDs are obtained using epitaxial superlattices, our results indicate that grain boundary variation within nanodots is not the primary origin of SFD broadening that occurs with nanopatterning. © 2007 American Institute of Physics. [DOI: 10.1063/1.2431399]

I. INTRODUCTION

Perpendicularly magnetized nanopatterned arrays show promise as a mean to increase density of magnetic storage media to greater than 160 Gbits/cm² (1 Tbit/in.²). However, to make this technology possible, narrow switching field distributions (SFDs) within these nanopatterned arrays are needed. Highly exchange coupled systems, such as Co/Pd and Co/Pt multilayers, have long been studied due to the large perpendicular magnetization that results from the interface anisotropy.¹⁻⁶ In addition, the coercive fields of these layers are large and exhibit very sharp reversal fields, which are desired in media storage technology. However, as these Co/Pd and Co/Pt multilayers are patterned to submicrometer dimensions, the SFD broadens significantly. This broadening is not well understood, but has been attributed to several sources, including lithographic variations between nanodots,⁷ grain orientation and/or grain boundary variations within nanodots,⁸ and more recently, distributions of the anisotropy field.⁹ In this work, we show that the SFD in nanopatterned Co/Pd multilayers is a direct result of the material properties of the multilayers. By improving the multilayer stack we have been able to significantly narrow the relative SFD of nanodot arrays.

II. EXPERIMENT

Polycrystalline multilayer films were dc magnetron sputter deposited in 0.63 Pa (4.7 mTorr) Ar on thermally oxidized Si(001) wafers. Samples then had either a 3 nm Pd seed layer or a bilayer seed consisting of 3 nm Ta followed by 3 nm Pd deposited to promote a (111) texture. We will refer to polycrystalline samples with these two seed layers as the “Pd seed” and the “Ta seed.” Eight bilayers of Co/Pd were then deposited for all samples with a fixed Pd-to-Co thickness ratio of 2.9 followed by a 3 nm Pd protective layer.

Epitaxial Co/Pd superlattices were grown in a molecular beam epitaxy (MBE) system with a base pressure in the medium-to-low 10⁻⁹ Pa (10⁻¹¹ Torr). All layers were deposited via e-beam evaporation at a rate of 0.01 nm/s while rotating the substrate. To obtain smooth epitaxial layers, we first immersed prime grade Si(111) wafers in a 2% HF solution for approximately 1 min until the surface was hydrophobic. The wafer was then immediately loaded into the MBE chamber and heated to approximately 700 °C to obtain a (7×7) Si(111) surface reconstruction. This process was monitored by *in situ* reflection high energy electron diffraction (RHEED). To promote epitaxial growth, a 4 nm Cu seed layer was first grown at room temperature followed by a 3 nm Pd layer. The Co/Pd multilayer stack was then deposited and capped with 3 nm Pd. RHEED images taken at various stages during growth are given in Fig. 1.

We patterned 100 and 50 nm nanodot arrays using electron beam lithography with a Co-PMMA/PMMA (poly-methyl methacrylate) bilayer. After holes were patterned and developed, Al or Cr was subsequently evaporated followed by a lift-off process in acetone. The Al or Cr was used as an

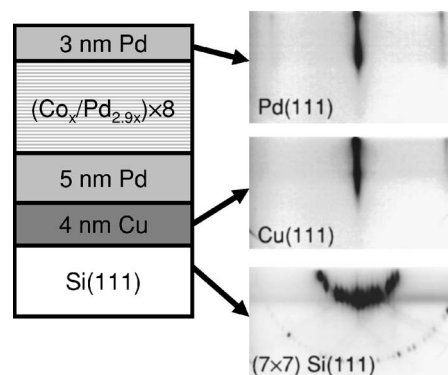


FIG. 1. (Color online) Structure of epitaxial Co/Pd superlattices with RHEED patterns of the initial (7×7) Si(111) surface (bottom), Cu(111) seed layer (middle), and Pd capping layer (top).

^{a)}Electronic mail: justin.shaw@nist.gov

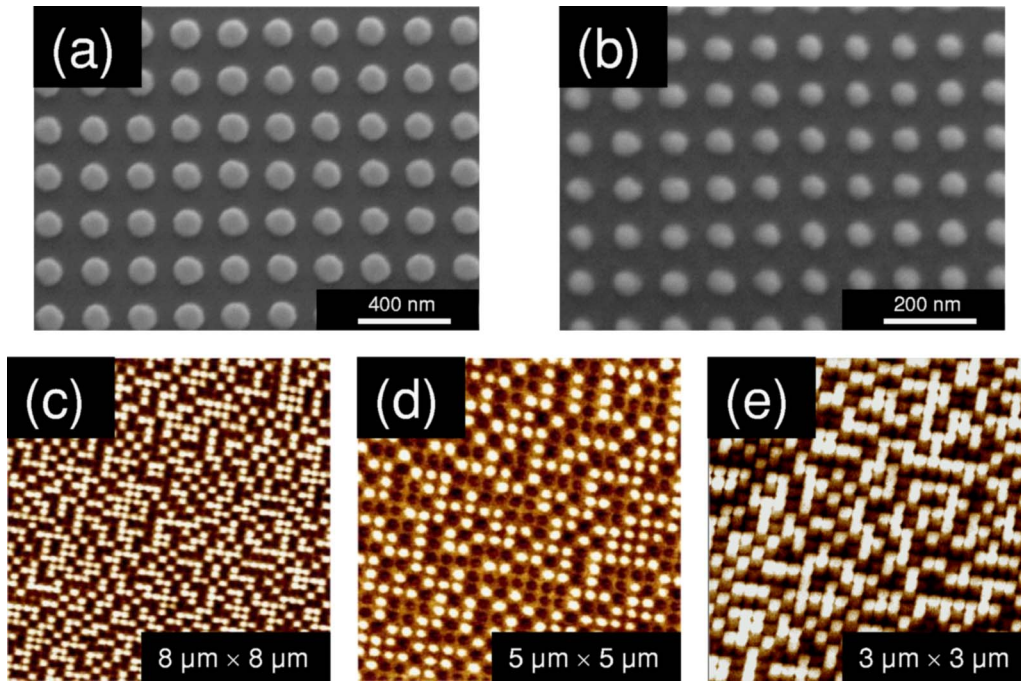


FIG. 2. (Color online) Scanning electron micrographs of (a) 100 nm diameter (200 nm pitch) and (b) 50 nm diameter (100 nm pitch) nanodot arrays. MFM images are also shown of the ac demagnetized state in epitaxial (c) 100 nm diameter (200 nm pitch), (d) 50 nm diameter (200 nm pitch), and (e) 50 nm diameter (100 nm pitch) nanodot arrays.

etch mask for ion milling the exposed Co/Pd regions, resulting in uniform arrays of nanodots, as shown in Figs. 2(a) and 2(b).

Remanent hysteresis curves for the nanodot arrays were obtained by counting the number of reversed dots in magnetic force microscopy (MFM) images in the remanent state after a static field was applied perpendicular to the sample surface for approximately 2 s. Figures 2(c)–2(e) show MFM images for 100 and 50 nm diameter dots with both 200 and 100 nm pitches (center-to-center spacing) after undergoing demagnetization. Strong coupling is not observed between nanodots in these images although some amount of coupling is unavoidable at these dimensions. The typical statistical samples for dot counting were 500–1000 for 100 nm diameter nanodots and 250–500 for 50 nm diameter nanodots.

III. RESULTS

Figure 3(a) shows alternating gradient magnetometry (AGM) hysteresis curves for several Co layer thicknesses in Pd seed, Ta seed, and epitaxial continuous films. The greatest difference among the AGM loops is the presence of an inflection point or a “tail” in the hysteresis curves for the Pd seed data. Our MFM measurements show that this tail results from localized regions of residual domains that require larger field than H_c to undergo annihilation. This behavior is commonly observed with perpendicular exchange coupled systems.^{1,2,10} It is important to note that this tail is most pronounced in the Pd seed layer samples, but also begins to appear in Ta seed layer samples with Co layer thicknesses greater than 0.35 nm. None of the epitaxial samples exhibit this behavior.

Although the relative layer thicknesses are identical in all samples, H_c varies significantly among the samples with a

Pd seed, Ta seed, and epitaxial superlattices, as shown in Fig. 3(b). Atomic force microscopy (AFM) reveals that the epitaxial superlattices have the highest rms roughness of 0.51–0.61 nm, followed by the Pd seed films with 0.22–0.25 nm, and the Ta seed with 0.18–0.23 nm. Any increase in roughness may provide pinning sites and account

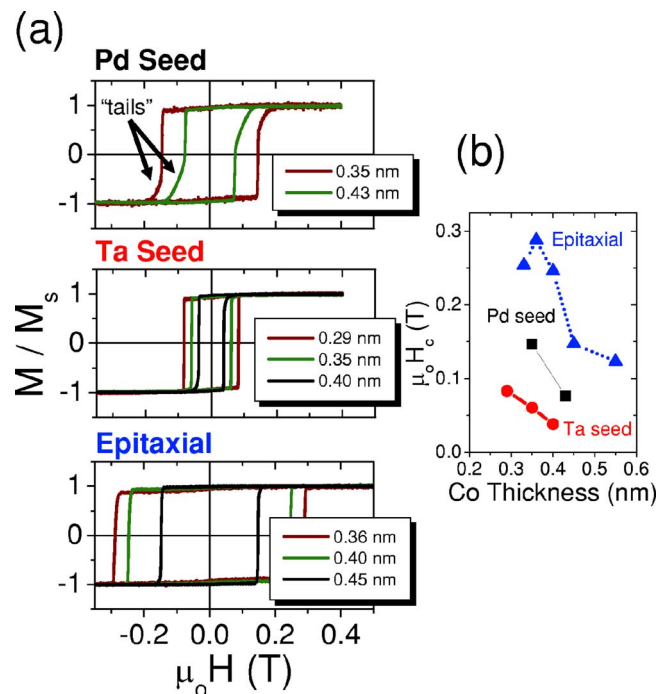


FIG. 3. (Color online) Out-of-plane AGM results on Co/Pd multilayer films showing (a) hysteresis curves of the Pd seed (top), Ta seed (middle), and epitaxial superlattice (bottom), and (b) the coercive field vs Co layer thickness in these films. The presence of the “tail” is most prevalent in the Pd seed layer hysteresis curve as indicated in the plot.

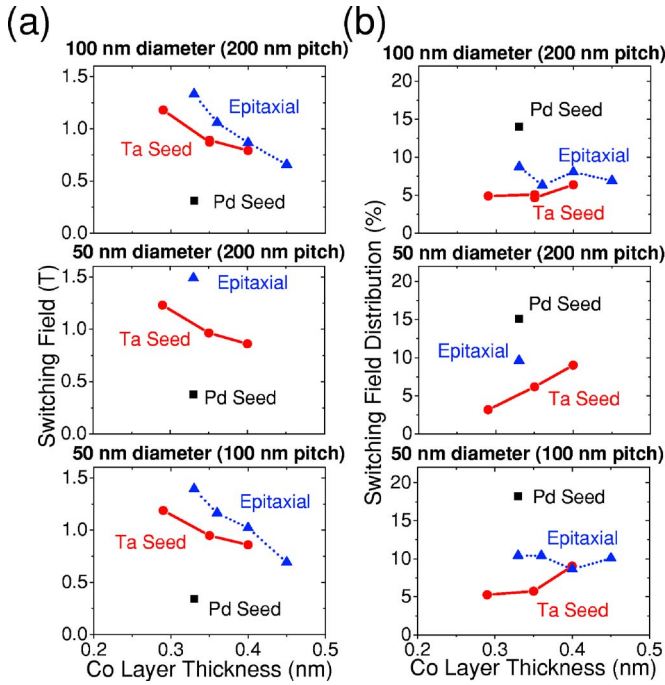


FIG. 4. (Color online) The switching fields versus Co layer thickness and (b) the switching field distribution versus Co layer thickness for the nanodot arrays. For both (a) and (b) the 100 nm diameter (200 nm pitch) data are given in the top plot, the 50 nm diameter (200 nm pitch) data are given in the middle plot, and those for the 50 nm diameter (100 nm pitch) arrays data are given in the bottom plot.

for the larger values of H_c for the corresponding films; however, the difference in roughness between the Pd seed and the Ta seed is minimal. The difference in structure between the polycrystalline and epitaxial films should not have a significant effect on the anisotropy since at these thicknesses it is dominated by the surface anisotropy, which is independent of film structure and orientation.³

Relative to the continuous film, the average switching field (H_{sf}) for the nanodot arrays increases substantially, as shown in Fig. 4(a). The approximate factors for this increase are 2.5 for Pd seed layers, 14–22 for Ta seed layers, and 4–6 for the epitaxial superlattices. This increase in H_{sf} is a result of two different reversal mechanisms: the continuous film undergoes a domain nucleation and domain wall propagation event, whereas the nanodots undergo Stoner-Wohlfarth reversal (i.e., coherent rotation), since they are single domains and have additional shape anisotropy.¹¹

Values of H_{sf} for nanodot arrays are taken as the field where 50% of the dots have undergone reversal. This is determined by fitting the integrated Gaussian distribution to the remanent hysteresis curves. Examples of the experimental and fitted data are shown in Fig. 5, where H_{sf} is normalized to unity. These data clearly show the Ta seed layer undergoing a sharp reversal with a dramatic reduction in relative SFD with respect to the other samples.

As a means of quantifying the SFD, we report values of the standard deviation of the Gaussian fit as a percentage of the H_{sf} and is plotted in Fig. 4(b). The broadest SFD is observed in the Pd seed layer arrays, which have been almost exclusively used in previous studies.^{9,11,12} The epitaxial superlattice arrays show a significant improvement in the SFD

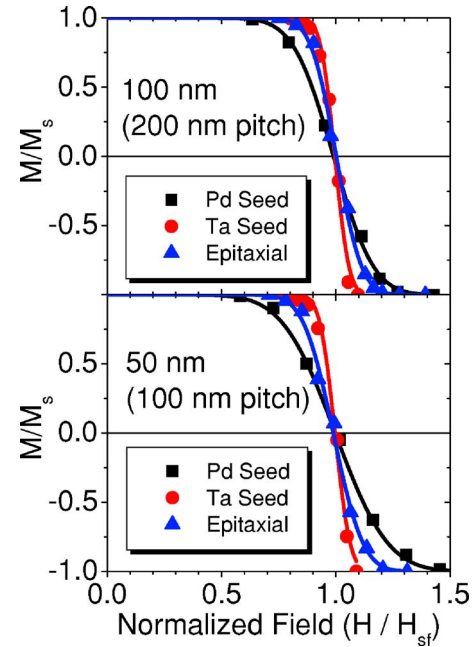


FIG. 5. (Color online) Examples of remanent state hysteresis curves obtained via MFM (data points) with the integrated Gaussian distribution fitted data (smoothed line) for 100 nm diameter (200 nm pitch) arrays (top), and 50 nm diameter (100 nm pitch) arrays (bottom). The Ta seed samples have narrow SFDs.

relative to Pd seed arrays. However, the Ta seed samples have a further reduction in SFD to below 5% for the thinnest Co layer thickness.

The relative or normalized SFD is more informative in comparing the switching behavior among the different materials and structures since it is analogous to the squareness ratio in hysteresis loops. However, for technological applications such as write head design in patterned media, absolute values of the SFD are also of interest. A plot of the absolute SFD as a function of the average switching field is given in Fig. 6.

IV. DISCUSSION

The SFD is correlated with the presence of the tail in the AGM hysteresis curves (Fig. 3) of the corresponding continuous films, especially within a given multilayer system.

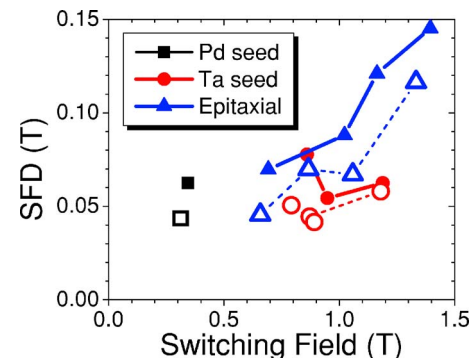


FIG. 6. (Color online) Absolute values of SFD as a function of the average switching field. The open data point with dashed lines are 100 nm diameter (200 nm pitch) arrays and the closed data points with solid lines are 50 nm diameter (100 nm pitch).

The Pd seed sample has both a broad SFD and a large tail in the film hysteresis curves. The hysteresis curves in the Ta seed samples start out extremely sharp for the lowest Co layer thicknesses and show no evidence of the tail. At thicker Co layer thicknesses, the SFD gradually increases and a small tail begins to appear in the corresponding continuous film hysteresis curves. On the other hand, the epitaxial SFD data are relatively constant for all Co layer thicknesses and the hysteresis curves of the continuous films are sharp and lack a tail. As a more general observation, the sharpness of magnetic reversal of the continuous films results in narrower SFDs for the various structures studied in this work. Thus, the magnetic behavior of the continuous film is strongly correlated with the magnetic behavior and SFD of the resulting nanopatterned structure. This suggests that the SFD originates primarily as a material or structural property within the multilayer and is not a consequence of lithographic variation since all our samples had identical lithographic processing. However, it is important to note that additional SFD broadening will occur if significant lithographic variations are present since H_{sf} is a function of nanodot diameter, as shown in Fig. 4(a).

Our results are further supported by Thomson *et al.*⁹ who found that an intrinsic distribution of anisotropy fields throughout their films can account for the broadening in SFDs after nanopatterning. One source of an intrinsic distribution of anisotropy could come from variations in grain structure, orientation, or grain boundaries. However, our epitaxial nanodots also exhibit significant SFD broadening with nanopatterning. The use of epitaxial structures isolates the influence of grain boundaries since each nanodot is a single grain with identical orientation. In addition, significant reduction in the SFD is achieved with polycrystalline Ta seed structures. These results indicate that grain boundary variation is not fundamentally the primary source of SFDs, as previously reported.⁸

The interfacial quality or roughness of the multilayers could also give rise to this distribution of nucleation fields. However, the difference in rms roughness between the Ta seed and the Pd seed arrays is minimal, yet the difference in SFDs is large. The epitaxial samples which have a significantly larger value of surface roughness have an intermediate value of SFD. Thus, there is no direct correlation between surface roughness and SFD. However, increased surface roughness could contribute additional SFD broadening since the surface/interface topography would vary between nanodots.

Finally, we speculate that the source of anisotropy distribution could come from variations in strain across the multilayer since both polycrystalline and epitaxial multilayers are strongly susceptible to strain, and it was recently

shown that the anisotropy may be dominated by strain for this system.¹³ All three structures (Pd seed, Ta seed, and epitaxial) used in this study could have significant and varying amounts of strain introduced into the multilayer due to the various seed layers and substrates used. Although beyond the scope of this work, a detailed study on the influence of strain on reversal properties of Co/Pd multilayers and resulting nanostructures is needed.

V. SUMMARY

In summary, we have fabricated Co/Pd nanodot arrays down to 50 nm in diameter that have SFDs below 5%. The use of a Ta seed layer in polycrystalline Co/Pd multilayers dramatically reduces the SFD relative to a conventional Pd seed layer. In addition, nanodot arrays fabricated from epitaxial Co/Pd superlattices exhibit a broadening in the SFD, indicating that the presence of grain boundaries is not the primary source of SFD broadening. Lithographic variations were also not found to be the primary cause of SFDs. Although these two factors could contribute additional broadening of the SFD, we find that the primary source of SFDs is due to an intrinsic material property of the Co/Pd multilayer.

ACKNOWLEDGMENTS

We are grateful to Bruce Terris for his advice and valuable discussions, Tsai-Wei Wu for providing dot reversal counting software, Kevin Garello for programming help, and Ross Potoff for his technical support. T.R. and C.M.F. were supported by DOE Grant No. DE-FG03-93ER45488. This work is an official contribution of the National Institute of Standards and Technology.

¹H. J. G. Draaisma, W. J. M. de Jonge, and F. J. A. den Broeder, *J. Magn. Mater.* **66**, 351 (1987).

²W. B. Zeper, F. J. A. M. Greidanus, P. F. Carcia, and C. R. Fincher, *J. Appl. Phys.* **65**, 4971 (1989).

³B. N. Engel, C. D. England, R. A. Van Leeuwen, M. H. Wiedmann, and C. M. Falco, *Phys. Rev. Lett.* **67**, 1910 (1991).

⁴S. E. Russek and W. E. Bailey, *IEEE Trans. Magn.* **36**, 2990 (2000).

⁵D. Weller, L. Folks, M. Best, E. E. Fullerton, B. D. Terris, G. J. Kusinski, K. M. Krishnan, and G. Thomas, *J. Appl. Phys.* **89**, 7525 (2001).

⁶H. Nemoto and Y. Hosoe, *J. Appl. Phys.* **97**, 10J109 (2005).

⁷Y. Kitade, H. Komoriya, and T. Maruyama, *IEEE Trans. Magn.* **40**, 2516 (2004).

⁸C. Haginoya, S. Heike, M. Itabashi, K. Nakamura, and K. Koike, *J. Appl. Phys.* **85**, 8327 (1999).

⁹T. Thomson, G. Hu, and B. D. Terris, *Phys. Rev. Lett.* **96**, 257204 (2006).

¹⁰J. E. Davies, O. Hellwig, E. E. Fullerton, G. Denbeaux, J. B. Kortright, and K. Liu, *Phys. Rev. B* **70**, 224434 (2004).

¹¹G. Hu, T. Thomson, C. T. Rettner, S. Raoux, and B. D. Terris, *J. Appl. Phys.* **97**, 10J702 (2005).

¹²B. D. Terris, M. Albrecht, G. Hu, T. Thomson, and C. T. Rettner, *IEEE Trans. Magn.* **41**, 2822 (2005).

¹³J. I. Hong, S. Sankar, A. E. Berkowitz, and W. F. Egelhoff, *J. Magn. Mater.* **285**, 359 (2005).